

Matter-wave interferometry in a double well on an atom chip

T. Schumm,^{1,2} S. Hofferberth,¹ L. M. Andersson,¹ S. Wildermuth,¹
S. Groth,^{1,3} I. Bar-Joseph,³ J. Schmiedmayer,^{1,*} and P. Krüger^{1,4,†}

¹*Physikalisches Institut, Universität Heidelberg, D-69120 Heidelberg, Germany*

²*Laboratoire Charles Fabry de l'Institut d'Optique, UMR 8105 du CNRS, F-91403 Orsay, France*

³*Department of Condensed Matter Physics, The Weizmann Institute of Science, Rehovot 76100, Israel*

⁴*Current address: Laboratoire Kastler Brossel, École Normale Supérieure, F-75005 Paris, France*

(Dated: February 1, 2008)

Matter-wave interference experiments enable us to study matter at its most basic, quantum level and form the basis of high-precision sensors for applications such as inertial and gravitational field sensing. Success in both of these pursuits requires the development of atom-optical elements that can manipulate matter waves at the same time as preserving their coherence and phase. Here, we present an integrated interferometer based on a simple, coherent matter-wave beam splitter constructed on an atom chip. Through the use of radio-frequency-induced adiabatic double-well potentials, we demonstrate the splitting of Bose-Einstein condensates into two clouds separated by distances ranging from 3 to 80 μm , enabling access to both tunnelling and isolated regimes. Moreover, by analysing the interference patterns formed by combining two clouds of ultracold atoms originating from a single condensate, we measure the deterministic phase evolution throughout the splitting process. We show that we can control the relative phase between the two fully separated samples and that our beam splitter is phase-preserving.

PACS numbers: 39.90.+d, 03.75.Be

The wave nature of matter becomes visible in interference experiments [1]. Interferometry with atoms has become an important tool for both fundamental and applied experiments in the diverse fields of atomic physics, quantum optics, and metrology [2]. For example, highly accurate acceleration measurements have been based on atom interference [3]. Even though in most cases, interference is fundamentally a single particle phenomenon, the experiments become even more powerful when performed with Bose-Einstein condensates (BECs). Interferometry was used to demonstrate the remarkable property of atoms in a BEC to possess a common phase [4]. Realizing miniaturized matter-wave interferometers, as well as controlling and engineering quantum states on a microscale in general, have been long standing goals. Microscopic integrated matter-wave devices [5] can be used to study the physics of correlated many-body quantum systems and are promising candidates for the implementation of scalable quantum information processing [6].

The combination of well-established tools for atom cooling and manipulation with state-of-the-art microfabrication technology has led to the development of atom chips [5, 7, 8, 9, 10]. These devices have been shown to be capable of trapping and guiding ultracold atoms on a microscale. A variety of complex manipulation potentials have been formed using magnetic [11], electric [12], and optical fields [13]. BECs can be created efficiently in such microtraps and coherent quantum phenomena such as internal-state Rabi oscillations [14] and coherent splitting in momentum space [15, 16] have been observed.

It is of particular interest to control the external (motional) degrees of freedom of trapped atoms and spatially delocalized wave packets on a quantum level [17, 18]. A

generic configuration for studies of matter-wave dynamics is the double well [19, 20]. Dynamically splitting a single trap into a double well is analogous to a beam splitter in optics and hence forms a basic element of a matter-wave interferometer. Interferometers on a microchip can be used as highly sensitive devices because they allow measurements of quantum phases. This enables experiments exploring the intrinsic phase dynamics in complex interacting quantum systems (for example, Josephson oscillations [20, 21]) or the influence of the coupling to an external 'environment' (decoherence [22]). Technologically, chip-based atom interferometers promise to be very useful as inertial sensors on a microscale [23]. For all these applications it is imperative that the deterministic coherent quantum evolution of the matter waves is not perturbed by the splitting process itself. Although several atom chip beam-splitter configurations have been proposed and experimentally demonstrated [12, 24, 25, 26, 27] none of them has fulfilled this crucial requirement.

We present an easily implementable scheme for a phase preserving matter-wave beam splitter. We demonstrate experimentally, for the first time, coherent spatial splitting and subsequent stable interference of matter waves on an atom chip. Our scheme is exclusively based on a combination of static and radio-frequency (RF) magnetic fields forming an adiabatic potential [28]. The atomic system in the combined magnetic fields can be described by a hamiltonian with uncoupled adiabatic eigenstates, so-called dressed states. For sufficiently strong amplitudes of the RF field, transitions between the adiabatic levels are inhibited as the strong coupling induces large repulsion of these levels. This property of the combined

static and RF fields could be exploited to form trapping geometries using the effective potential acting on the dressed eigenstates [29], and related demonstration experiments with thermal atoms have been performed [30].

In a more general case than considered in ref. [29], the orientation, in addition to the intensity and frequency, of the RF field determine the effective adiabatic potential V_{eff} at the position \mathbf{r} :

$$V_{\text{eff}}(\mathbf{r}) = \frac{m_F \sqrt{[\mu_B g_F B_{\text{d.c.}}(\mathbf{r}) - \hbar \omega_{\text{RF}}]^2 + [\mu_B g_F B_{\text{RF}\perp}(\mathbf{r})/2]^2}}{m_F} \quad (1)$$

Here m_F is the magnetic quantum number of the state, g_F is the Landé factor, μ_B is the Bohr magneton, \hbar is the reduced Planck's constant, $B_{\text{d.c.}}$ is the magnitude of the static trapping field and ω_{RF} is the frequency of the RF field. $B_{\text{RF}\perp}$ is the amplitude of the component of the RF field perpendicular to the local direction of the static trapping field. The directional dependence of this term implies the relevance of the vector properties of the RF field, which enables the formation of a true double-well potential.

Figure 1 illustrates the operation principle of the beam splitter. A standard magnetic microtrap [5] is formed by the combined fields of a current-carrying trapping wire and an external bias field; a static magnetic field minimum forms where atoms in low-field-seeking states can be trapped. An RF field generated by an independent wire carrying an alternating current couples internal atomic states with different magnetic moments. Owing to the strong confinement in a microtrap, the angle between the RF field and the local static magnetic field varies significantly over short distances, resulting in a corresponding local variation of the RF coupling strength. By slowly changing the parameters of the RF current we smoothly change the adiabatic potentials and transform a tight magnetic trap into a steep double well, thereby dynamically splitting a BEC without exciting it. We accurately control the splitting distance over a wide range. The potential barrier between the two wells can be raised gradually with high precision, thus enabling access to the tunnelling regime [20] as well as to the regime of entirely isolated wells.

The beam splitter is fully integrated on the atom chip, as the manipulating potentials are provided by current-carrying microfabricated wires. The use of chip-wire structures allows one to create sufficiently strong RF fields with only moderate currents and permits precise control over the orientation of the RF field. Note that in our configuration the magnetic near-field part of the RF field completely dominates.

We complete the interferometer sequence and measure the relative phase between the split BECs by recombining the clouds in time-of-flight expansion. In our ex-

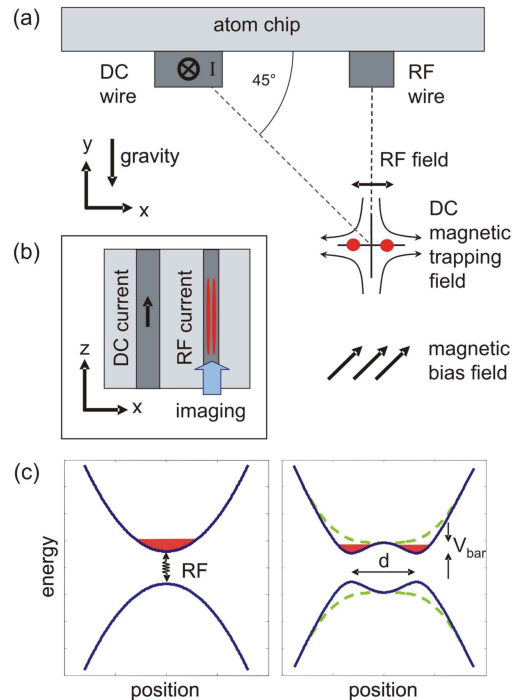


FIG. 1: Operation principle of the beam splitter. (a), A straight wire carrying a static (d.c.) current (~ 1 A) is used to trap a BEC on an atom chip directly below a second wire carrying a RF current (~ 60 mA at 500 kHz). The d.c. wire has a width of $50 \mu\text{m}$, it is separated by $80 \mu\text{m}$ from the RF wire (width $10 \mu\text{m}$). Placing the trap $80 \mu\text{m}$ from the chip surface at the indicated position allows for symmetric horizontal splitting. (b), Top view onto the atom chip (mounted upside down in the experiment): an elongated BEC is transversely split. All images are taken along the indicated direction. (c), Left: The RF magnetic field couples different atomic spin states (only two shown for simplicity). Right: the initial d.c. trapping potential is deformed to an effective adiabatic potential under the influence of the RF field with a frequency below the Larmor frequency at the trap minimum (~ 1 G). In the vertical (y) direction, the spatially homogeneous RF coupling strength leads to a slight relaxation of the static trap (dashed green line). Along the horizontal (x) direction, the additional effect of local variations of the RF coupling breaks the rotational symmetry of the trap and allows for the formation of a double-well potential with a well separation (d) and potential barrier height V_{bar} (solid blue line).

periments we found an interference pattern with a fixed phase as long as the two wells are not completely separated. The phase distribution remains non-random and its centre starts to evolve deterministically once the wells are entirely separated so that tunnelling is fully inhibited on all experimental timescales.

The experiments are performed in the following way. We routinely prepare BECs of up to $\sim 10^5$ rubidium-87

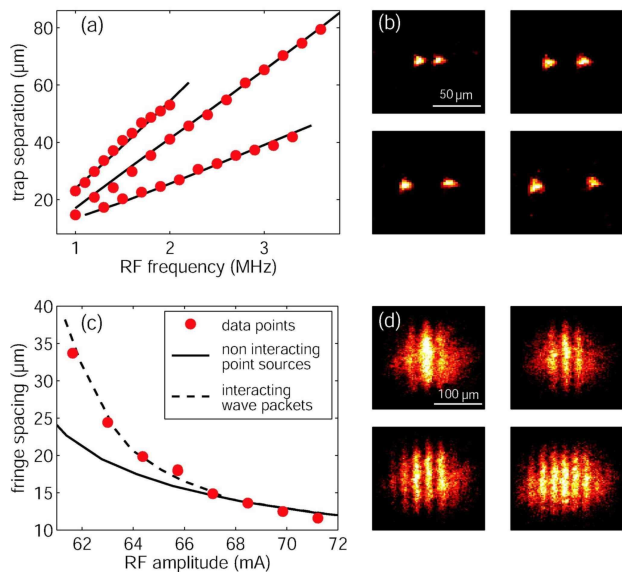


FIG. 2: The splitting of BECs is controlled over a wide spatial range. By adjusting amplitude and frequency of the RF field, we have been able to reach splitting distances of up to $80 \mu\text{m}$. (a), A comparison of the measured splitting distances (red circles) to the theoretical expectation (black lines) yields good agreement for three different strengths of transverse confinement (gradients 1.1 , 1.9 and 2.4 kG cm^{-1} , top to bottom). (b), The experimental data are derived from *in situ* absorption images (Roper Scientific MicroMAX: 1024BFT). (c), The fringe spacing is plotted as a function of RF amplitude (red circles). A simple approximation of the expected fringe spacing based on an expansion of a non-interacting gas from two points located at the two double-well minima agrees well with the data for sufficiently large splittings (solid line). For small splitting distances (large fringe spacings), inter-atomic interactions affect the expansion of the cloud. A numerical integration of the time-dependent Gross-Pitaevskii equation using our experimental parameters takes this effect into account (dotted line). (d), Interference patterns obtained after 14 ms potential-free time-of-flight expansion of the two BECs. For splittings below our imaging resolution ($d < 6 \mu\text{m}$), the splitting distances can be derived from these interference patterns.

atoms in the $F = m_F = 2$ hyperfine state in microtraps near the surface of an atom chip [31]. Our smooth microwires [32] enable us to create pure one-dimensional condensates (aspect ratio ~ 400) with chemical potential $\mu \sim \hbar\omega_{\perp}$ in a trap with high transverse confinement ($\omega_{\perp} = 2\pi \times 2.1 \text{ kHz}$) [33, 34]. By tilting the external bias field, we position the BECs directly below an auxiliary wire (Fig. 1). A small sinusoidally alternating current through this wire provides the RF field that splits the trap. For small splitting distances ($< 6 \mu\text{m}$) we ramp the amplitude of the RF current from zero to its final value (typically 60 - 70 mA) at a constant RF frequency ($\sim 500 \text{ kHz}$). This frequency is slightly below the Larmor frequency of the atoms at the minimum of the static

trap ($\sim 1 \text{ G}$ corresponding to $\sim 700 \text{ kHz}$). By applying the ramp, we smoothly split a BEC confined in the single-well trap into two. The splitting is performed transversely to the long axis of the trap, as shown in Fig. 1b. The distance between the two wells can be further increased by raising the frequency of the RF field (up to 4 MHz in our experiment). The atoms are detected by resonant absorption imaging (see Fig. 2) along the weak trapping direction, that is, integrating over the long axis of the one-dimensional clouds. The images are either taken *in situ* or after time-of-flight expansion.

Unbalanced splitting can occur owing to the spatial inhomogeneity of the RF field, owing to asymmetries in the static magnetic trap and owing to gravity. Although the splitting process itself is very robust, imbalances lead to a rapid evolution of the relative phase of the two condensates once they are separated. The influence of gravity can be eliminated by splitting the trap horizontally. In the experiment we balance the double well by fine-tuning the position of the original trap relative to the RF wire.

To characterize the splitting, the split cloud is detected *in situ*. We are able to split BECs over distances of up to $80 \mu\text{m}$ without significant loss or heating (determined in time-of-flight imaging). The measured splitting distances are in very good agreement with the theoretical expectations for different configurations of the initial single well (Fig. 2a).

To study the coherence of the splitting process we recombine the split clouds in time-of-flight expansion after a non-adiabatically fast ($< 50 \mu\text{s}$) extinction of the double-well potential. Typical matter-wave interference patterns obtained by taking absorption images 14 ms after releasing the clouds are depicted in Figure 2d. The transverse density profile derived from these images contains information on both the distance d of the BECs in the double-well potential and the relative phase ϕ of the two condensates. We determine the fringe spacing Δz and the phase ϕ by fitting a cosine function with a Gaussian envelope to the measured profiles (Fig. 3). For large splittings ($d > 5 \mu\text{m}$ for our experimental parameters), the fringe spacing is given by $\Delta z = \hbar t / md$, where \hbar is Planck's constant, t is the expansion time and m is the atomic mass. This approximation of a non-interacting gas expanding from two point sources is inaccurate for smaller splittings where the repulsive interaction in the BEC has to be taken into account [35]. Figure 2c shows the observed fringe spacing that is compared with the above approximation and with a numerical integration of the time-dependent Gross-Pitaevskii equation. We find excellent agreement with the latter theory.

We assess the coherence properties of the beam splitter by analysing the relative phase between the two condensates throughout the splitting process. Figure 3 shows the results for 40 repetitions of the interference experiment performed directly after the two condensates are separated (Fig. 3a) and after they have been taken far-

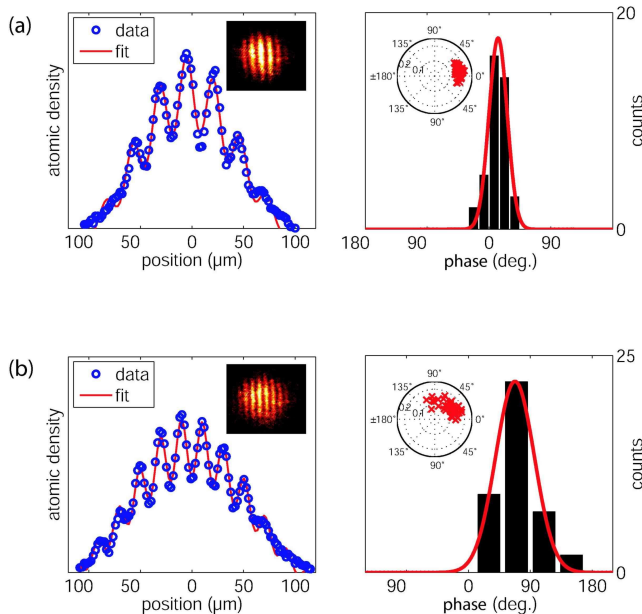


FIG. 3: The coherence of the splitting is examined by analysing matter-wave interference patterns. (a), Directly after (0.1 ms) the BECs have been split far enough ($d = 3.4 \mu\text{m}$) to inhibit tunnelling completely. (b), After (0.8 ms) the clouds have been taken farther apart ($d = 3.85 \mu\text{m}$). Left: a cosine function with a Gaussian envelope is fitted to the profiles derived from the two-dimensional images (insets). This yields information on fringe spacing, contrast and phase. Right: contrast and relative phase for 40 realizations of the same experiment are plotted in a polar diagram (inset). A histogram of the same data shows a very narrow distribution of the differential phase ($\sigma = 13^\circ$) directly after separating the clouds and a slightly broadened distribution ($\sigma = 28^\circ$) later in the splitting process. Both phase spreads are significantly smaller than what is expected for a random phase.

ther apart (Fig. 3b), respectively. We find a very narrow phase distribution with a Gaussian width of $\sigma = 13^\circ$ and 28° , respectively. Hence, the splitting process is phase-preserving and the beam splitter is coherent.

We have performed similar measurements throughout the entire splitting process, starting from a well separation of $d \sim 3 \mu\text{m}$ where the BECs are still connected to a splitting of $d \sim 5.5 \mu\text{m}$. At larger d , the interference fringes are no longer optically resolved. For splitting distances larger than $3.4 \mu\text{m}$ the potential barrier is sufficiently high to suppress tunnel coupling between the two wells, so that the splitting process is complete. For fast splitting we find the phase distribution to be non-random over the whole splitting range (Fig. 4a). In a more detailed experiment with slower splitting we find that the spread is smaller than the expectation of a randomized phase by more than three standard deviations for splitting times shorter than 2 ms (Fig. 4c). Within these limits, our data show an increase in phase spread and a

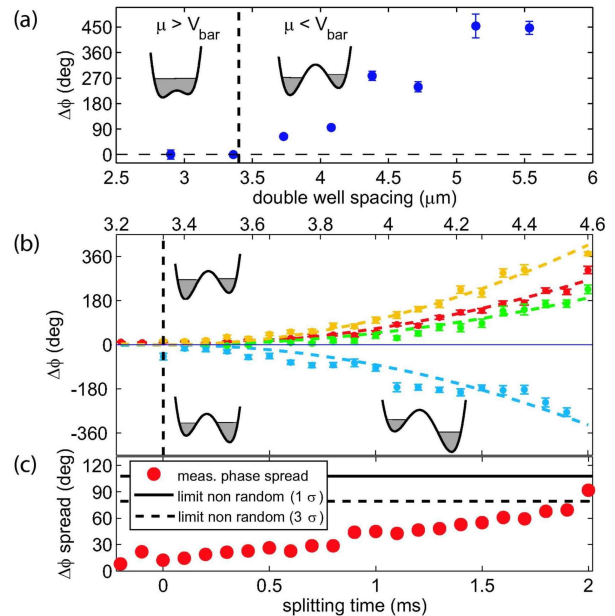


FIG. 4: Evolution of the differential phase throughout the splitting process. Error bars indicate the statistical error of the mean value. (a), Splitting the condensate to variable distances within 12 ms (splitting speed $1.4 \mu\text{m ms}^{-1}$). The dashed vertical line indicates the trap separation for which the chemical potential μ of the BEC equals the potential barrier height V_{bar} ($3.4 \mu\text{m}$). As long as the barrier between the two wells is sufficiently low (left of the dashed line), the relative phase remains locked at zero. Once the wells are fully separated so that tunnelling is inhibited (right of the dashed line), the differential phase starts to evolve owing to a slight residual imbalance in the double well. (b), Relative phase of the two condensates throughout a slower splitting process (splitting speed $0.6 \mu\text{m ms}^{-1}$). The evolution of the differential phase is controlled by deliberately adjusting the double-well imbalance by displacing the trap. The observed evolution is in agreement with a numerical simulation based on our experimental parameters (dashed lines) for all data sets (yellow, red, green and blue points). Both signs of imbalance have been realized and the phase evolution is observed for a time (2 ms), which is more than four times the transverse oscillation period. (c), A typical distribution of the relative phase shows significantly non-random phases for the entire splitting process, the limits for a deviation by one and three standard deviations are indicated.

coinciding loss of average contrast. A possible explanation is the longitudinal phase diffusion inside the individual one-dimensional quasi-BECs [36]. This hypothesis is supported by the fact that we always observe phase randomization (at finite interference contrast) approximately 2.5 ms after the splitting is complete, independent of the splitting distance d . This timescale roughly agrees with the theoretical prediction for our experimental parameters. More detailed experimental studies of the longitudinal phase diffusion inside one-dimensional quasi-BECs are underway.

As the splitting is a coherent operation, we are able to measure the phase evolution throughout the splitting process. We find that the relative phase between the two condensates is locked to zero as long as the chemical potential exceeds the potential barrier ($d < 3.4 \mu\text{m}$). Once the splitting is complete ($d > 3.4 \mu\text{m}$), a deterministic phase evolution occurs (Fig. 4a,b). A differential phase shift is induced by a slight residual imbalance of the double-well potential (in the case shown in Fig. 4a an energy difference of the order of $h \times 1 \text{ kHz } \mu\text{m}^{-1}$ additional splitting).

The double-well imbalance can be controlled by appropriately adjusting the trap parameters. In our experiment we have studied this by varying the current in the d.c. trapping wire and thereby adjusting the position of the original single-well trap with respect to the RF wire and the orientation of the splitting axis with respect to gravity. The data depicted in Fig. 4b show the resulting phase evolution for four different settings. Again, the differential phase ϕ is zero as long as the clouds are not fully separated; once tunnelling is inhibited, ϕ evolves quadratically with the split time. Although the differential phase evolution in an asymmetric double well is usually linear in time, in our case the wells are separated further as the split time is increased, so that the imbalance itself increases linearly with time. This leads to an overall quadratic scaling, which is confirmed by a numerical integration of the time-dependent Gross-Pitaevskii equation. We have varied both the sign and strength of the imbalance in the double-well potential. It is a crucial property of our beam splitter that the balancing is fairly insensitive to changes of the controlling parameter. The balancing can then be performed well above the experimental noise level. In the illustrated case we have varied the d.c. wire current on the per cent level ($\sim 10 \text{ mA}$ corresponding to a trap displacement of $\sim 1 \mu\text{m}$), whereas the current stability is better than 10^{-4} . In our experiment, we have been able to balance the double well to an extent that within one transverse oscillation period (0.5 ms) after the condensates were fully separated, the phase shift remained smaller than 18° .

There are several advantages of our atom chip beam-splitter concept over previously implemented approaches: the splitting distances are not limited by the structure size on the chip [37], but rather by the ground-state size of the initial single-well trap that can be orders of magnitude smaller. This allows us to reach full splitting of a BEC of $1.1 \mu\text{m}$ transverse size (full width at half maximum) at a double-well separation of only $3.4 \mu\text{m}$. The trapping wire, in contrast, has a width of $50 \mu\text{m}$; the atoms are located at a distance of $80 \mu\text{m}$ from the surface. Furthermore, the dynamic splitting process can be performed in a smooth (adiabatic) fashion, avoiding excitations, by simply controlling the parameters of the RF field.

In conclusion, we have demonstrated coherent splitting

and interference of BECs using an atom chip. Our experiments are based on a versatile microfabricated beam splitter that is fully integrated on the chip. With our interferometer we have measured and controlled the phase evolution between two BECs gradually split over increasingly large distances. We are convinced that such double-well potentials on atom chips are a starting point for a variety of in-depth studies of the dynamics of one- and three-dimensional quantum gases. Exploring the splitting and recombination process in more detail is an immediate next step, as are detailed studies of tunnelling and self-trapping in low-dimensional quantum gases [20, 38]. Of particular interest will be the time-dependent evolution and phase coherence along low-dimensional correlated quantum systems in the fully split and in the tunnelling regimes. Applications of our scheme may range from investigations of atom-surface interactions and the fundamental question of surface-induced decoherence to microscopic atom interferometers for precision metrology. Last but not least, simple and robust atom chip beam splitters and interferometers based on our beam splitter may constitute the building blocks for quantum information processing on the atom chip [6, 17].

We thank H. Perrin and I. Lesanovsky for useful discussions. We acknowledge financial support from the European Union, contract numbers IST-2001-38863 (ACQP), MRTN-CT-2003-505032 (Atom Chips), HPRN-CT-2002-00304 (FASTNet), HPMF-CT-2002-02022, and HPRI-CT-1999-00114 (LSF) and the Deutsche Forschungsgemeinschaft, contract number SCHM 1599/1-1.

* Electronic address: schmiedmayer@atomchip.org

† Electronic address: krueger@physi.uni-heidelberg.de; URL: <http://www.atomchip.net>

- [1] G. Badurek, H. Rauch, and A. Zeilinger, eds., *Matter Wave Interferometry* (North Holland Physics Publishing Division, Amsterdam, 1988).
- [2] P. Berman, ed., *Atom Interferometry*, vol. 37 of *Adv. At. Mol. Opt. Phys.* (Academic Press, New York, 1997).
- [3] M. Kasevich and S. Chu, *Phys. Rev. Lett.* **67**, 181 (1991).
- [4] M. R. Andrews, C. G. Townsend, H.-J. Miesner, D. S. Durfee, D. M. Kurn, and W. Ketterle, *Science* **275**, 637 (1997).
- [5] R. Folman, P. Krüger, J. Schmiedmayer, J. Denschlag, and C. Henkel, *Adv. At. Mol. Opt. Phys.* **48**, 263 (2002).
- [6] M. A. Cirone, A. Negretti, T. Calarco, P. Krger, and J. Schmiedmayer (2005), published online DOI: 10.1140/epjd/e2005-00175-8.
- [7] D. Müller, D. Z. Anderson, R. J. Grow, P. D. D. Schwindt, and E. A. Cornell, *Phys. Rev. Lett.* **83**, 5194 (1999).
- [8] J. Reichel, W. Hänsel, and T. W. Hänsch, *Phys. Rev. Lett.* **83**, 3398 (1999).
- [9] R. Folman, P. Krüger, D. Cassettari, B. Hessmo, T. Maier, and J. Schmiedmayer, *Phys. Rev. Lett.* **84**, 4749 (2000).

- [10] N. H. Dekker, C. S. Lee, V. Lorent, J. H. Thywissen, S. P. Smith, M. Drndić, R. M. Westervelt, and M. Prentiss, *Phys. Rev. Lett.* **84**, 1124 (2000).
- [11] K. Brugger, P. Krüger, X. Luo, S. Wildermuth, H. Gimpel, M. W. Klein, S. Groth, R. Folman, I. Bar-Joseph, and J. Schmiedmayer, *Phys. Rev. A* **72**, 023607 (2005).
- [12] P. Krüger, X. Luo, M. W. Klein, K. Brugger, A. Haase, S. Wildermuth, S. Groth, I. Bar-Joseph, R. Folman, and J. Schmiedmayer, *Phys. Rev. Lett.* **91**, 233201 (2003).
- [13] R. Dumke, T. Mütther, M. Volk, W. Ertmer, and G. Birkl, *Phys. Rev. Lett.* **89**, 220402 (2002).
- [14] P. Treutlein, P. Hommelhoff, T. Steinmetz, T. W. Hänsch, and J. Reichel, *Phys. Rev. Lett.* **92**, 203005 (2004).
- [15] Y.-J. Wang, D. Z. Anderson, V. M. Bright, E. A. Cornell, Q. Diot, T. Kishimoto, M. Prentiss, R. A. Saravanan, S. R. Segal, and S. Wu, *Phys. Rev. Lett.* **94** (2005).
- [16] A. Günther, S. Kraft, M. Kemmler, D. Koelle, R. Kleiner, C. Zimmermann, and J. Fortagh (2005), [cond-mat/0504210](#).
- [17] T. Calarco, E. A. Hinds, D. Jaksch, J. Schmiedmayer, J. I. Cirac, and P. Zoller, *Phys. Rev. A* **61**, 022304 (2000).
- [18] E. Charron, E. Tiesinga, F. Mies, and C. Williams, *Phys. Rev. Lett.* **88**, 077901 (2002).
- [19] Y. Shin, M. Saba, T. A. Pasquini, W. Ketterle, D. E. Pritchard, and A. E. Leanhardt, *Phys. Rev. Lett.* **92**, 050405 (2004).
- [20] M. Albiez, R. Gati, J. Fölling, S. Hunsmann, M. Cristiani, and M. K. Oberthaler, *Phys. Rev. Lett.* **95**, 010402 (2005).
- [21] B. D. Josephson, *Physics Letters* **1**, 251 (1962).
- [22] W. H. Zurek, *Rev. Mod. Phys.* **75**, 715 (2003).
- [23] M. Kasevich, *Science* **298**, 1363 (2002).
- [24] D. Cassettari, B. Hessmo, R. Folman, T. Maier, and J. Schmiedmayer, *Phys. Rev. Lett.* **85**, 5483 (2000).
- [25] D. Müller, E. A. Cornell, M. Prevedelli, P. D. D. Schwindt, A. Zozulya, and D. Z. Anderson, *Opt. Lett.* **25**, 1382 (2000).
- [26] P. Hommelhoff, W. Hnsel, T. Steinmetz, T. W. Hnsch, and J. Reichel, *New Journal of Physics* **7**, 3 (2005).
- [27] Y. Shin, C. Sanner, G.-B. Jo, T. A. Pasquini, M. Saba, W. Ketterle, D. E. Pritchard, M. Vengalattore, and M. Prentiss (2005), [cond-mat/0506464](#).
- [28] E. Muskat, D. Dubbers, and O. Schöpf, *Phys. Rev. Lett.* **58**, 2047 (1987).
- [29] O. Zobay and B. M. Garraway, *Phys. Rev. Lett.* **86**, 1195 (2001).
- [30] Y. Colombe, E. Knyazchyan, O. Morizot, B. Mercier, V. Lorent, and H. Perrin, *Europhys. Lett.* **67**, 593 (2004).
- [31] S. Wildermuth, P. Krüger, C. Becker, M. Brajdic, S. Haupt, A. Kasper, R. Folman, and J. Schmiedmayer, *Phys. Rev. A* **69**, 030901(R) (2004).
- [32] S. Groth, P. Krüger, S. Wildermuth, R. Folman, T. Fernholz, D. Mahalu, I. Bar-Joseph, and J. Schmiedmayer, *Appl. Phys. Lett.* **85**, 2980 (2004).
- [33] P. Krüger, L. M. Andersson, S. Wildermuth, S. Hofferberth, E. Haller, S. Aigner, S. Groth, I. Bar-Joseph, and J. Schmiedmayer (2005), [cond-mat/0504686](#).
- [34] S. Wildermuth, S. Hofferberth, I. Lesanovsky, E. Haller, L. M. Andersson, S. Groth, I. Bar-Joseph, P. Krüger, and J. Schmiedmayer, *Nature* **435**, 440 (2005).
- [35] A. Röhl, M. Naraschewski, A. Schenzle, and H. Wallis, *Phys. Rev. Lett.* **78**, 4143 (1997).
- [36] N. K. Whitlock and I. Bouchoule, *Phys. Rev. A* **68**, 053609 (2003).
- [37] J. Estève, T. Schumm, J.-B. Trebbia, I. Bouchoule, A. Aspect, and C. I. Westbrook, *Eur. Phys. J. D* **35**, 141 (2005).
- [38] S. Giovanazzi, R. Shenoy, A. Smerzi, and S. Fantoni, *Phys. Rev. Lett.* **79**, 4950 (1997).